Gold nanorod photoluminescence : applications to imaging and temperature sensing

Carattino, A.

5

PLASMON DAMPING AS A FUNCTION OF TEMPERATURE

The fundamental property of metallic nanoparticles is the presence of a localized surface plasmon resonance. This resonance gives rise to very intriguing and useful properties such as sub-wavelength field confinement, increase in the efficiency of creation of hot carriers, large absorption and scattering cross sections. In this work we show that the plasmon resonance width increases linearly with temperature in the range from $293\,K$ *to* $350\,K$*. This can be used to measure temperature employing far field optics and can have many applications in different fields.*

5.1. INTRODUCTION

MEASURING temperature at the nanoscale is one of the main open challenges in biology[1], specially when focused into the promising fields of photothermal[2, 3] and photodynamic therapy[4]. The first method normally employs small nanoparticles to efficiently convert irradiation energy into heat in very localized environments[5], thus making it possible to address specific cells[3, 6]. The latter employs the nanoparticles as small antennas, utilizing the enhanced near field to produce singlet oxygen that in turn will induce cell apoptosis[7] or to induce drug delivery after irradiation[8].

Successfully designing and implementing new therapies requires not only a careful understanding of the mechanisms involved, but also needs tools to measure and validate the hypotheses. For instance, little is reported in literature regarding the critical temperatures needed for inducing cell death[2]. Much less is reported regarding the effect of a single nanoparticle in or in the vicinity of a cell.

Measuring temperature in cells has been recently subject to debate, mainly because measurements contradict the expected thermodynamic values[1, 9, 10]. Therefore new techniques that can shine light into these matters are very valuable. Moreover these techniques should be easy to implement in existing setups and ideally should not interfere with the environment to be measured.

Biologically relevant questions however are not the only open concerns regarding temperature at the nanoscale. For instance the temperature of a nanoparticle in an optical tweezer can be estimated from models[11] or by indirect measurements. Two different approaches include looking at the rotational diffusion coefficient[12] or by seeing changes in a lipid bilayer standing in the vicinity[5, 13]. These methods are specific to some experiments and can't be easily generalized.

The mentioned therapies are not the only research areas where nanoparticles have become very promising tools. In particular gold nanoparticles have been successfully employed as biosensors[14, 15], labels[16, 17], nanoantennas[18, 19] and are currently under investigation for solar energy conversion[20]. The main property for such broad range of applications resides in the presence of a localized surface plasmon resonance (LSPR) that strongly depends on the shape of the particles[21]. Normally this resonance will lie between 2.34 eV (530 nm) for spheres and in the near infrared for more elongated particles.

The plasmon resonance on one hand is responsible for high electromagnetic field enhancements near tips or protrusions[22, 23]. Because of this, nanoparticles currently are employed as nanometer-sized antennas useful both for Raman scattering (SERS)[24] and also for enhanced fluorescence[25, 26] experiments. On the other hand, the plasmon resonance energy is highly sensitive to the refractive index[27] of the medium surrounding the particles. This phenomenon is exploited for instance in nanosensors that rely in minute changes in the plasmon resonance to detect down to single molecules[14].

The energy (or equivalently the wavelength) of the resonance is not the only useful parameter for sensing applications. The resonance's width is also dependent on surrounding conditions[28, 29] and therefore can be exploited. In this work we propose the use of the FWHM of the resonance as a parameter to measure temperature changes of the immersion medium. In order to achieve a better understanding of the phenomenon it is important to determine the different parameters that explain the resonance's linewidth of

the plasmon.

In literature the main mechanisms involved in the description of the damping of the plasmon resonance are electron-phonon scattering, electron-surface scattering, radiative damping and electron-electron scattering[30–32]. Interband damping can be neglected if the resonance energies are low enough, which is the case for the nanorods we studied. Each one of the mentioned terms contributes additively to the total plasmon damping; electron-phonon scattering however is the only one that shows a strong dependence on temperature[28, 29]. From the Debye model of phonons and a Fermi distribution of the conduction electrons it is possible to calculate the damping term attributed to electron-phonon interaction $\Gamma_{\text{e-ph}}$ as[33],

$$\Gamma_{\text{e-ph}} = \frac{\hbar}{\tau_0}\left[\frac{2}{5} + 4\left(\frac{T}{\Theta_D}\right)^5 \int_0^{\Theta_D/T} \frac{z^4}{e^z - 1}\,\mathrm{dz}\right] \tag{5.1}$$

where $\tau_0 = 30\,\text{fs}$[28], $\Theta_D = 170\,\text{K}$[34]. It is important to note that this equation is valid in the case $T < \Theta_D$, in which mostly acoustic phonon modes are occupied. For temperatures $T > \Theta_D$ and by following a simple model for metals it is possible to simplify eqn. 5.1 into[35]

$$\Gamma_{\text{e-ph}} = \lambda \frac{k_\text{B} T}{\hbar} \tag{5.2}$$

where λ is a constant depending on the metal, and k_B is Boltzmann's constant. Equations 5.1 and 5.2 are derived in the limit $E_f \gg \hbar\omega \gg k_\text{B} T$, where E_f is the Fermi energy and $\hbar\omega$ is the plasmon resonance energy. For gold, $E_f = 5.53\,\text{eV}$, and at room temperature $k_\text{B} T = 0.026\,\text{eV}$. For nanoparticles with resonances at around 1.91 eV as the ones employed in this work, both conditions are satisfied. The coefficient λ is assumed to be a constant of the metal, but it could also be an intrinsic property of each particle.

Previous work done at low temperatures on bulk gold[33], gold nanorods[29] and gold bipyramids[28] showed a good agreement of the model in equation 5.1 with the experimental results. On average it was found that the electron-phonon damping increases with a rate of 0.1 meV/ K for temperatures above the Debye temperature, independently of the geometry. Nanorods or bipyramids normally have plasmon resonances below 2 eV and therefore interband damping mechanisms can be discarded. [36, 37]

Figure 5.1 shows white light scattering spectra of a single gold nanorod at 293 K and 333 K with the corresponding lorentzian fits. The plasmonic resonance centered around 1.857 eV is clearly visible. The FWHM of the fit at 333 K is 3.6 meV larger than at 293 K; this increase in width is of about 3% over a 40 K temperature change. The inset of the figure shows a SEM image of a cluster of the typical particles employed in this work.

Measuring the plasmonic resonance of single gold nanorods can be achieved not only by detecting white light scattering spectra but also by exciting their luminescence[29]. It has to be kept in mind, however, that measuring scattering spectra benefits from the enhanced cross section at the resonant wavelengths without being affected by the very low quantum yield of the luminescence[38]. This in turn will allow us to use much lower excitation powers and shorter acquisition times.

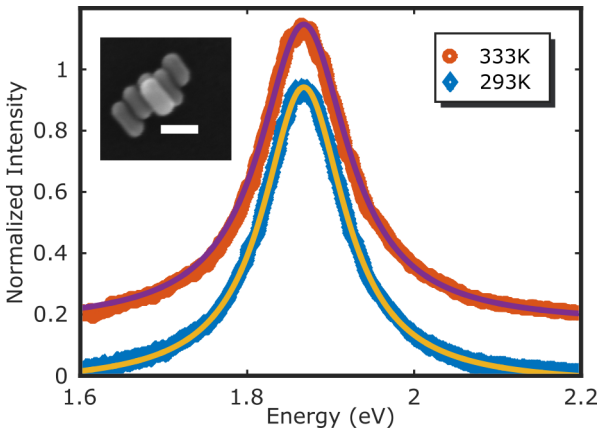

Figure 5.1: Normalized scattering spectra of a single gold nanorod at 293 K and at 333 K with corresponding lorentzian fits. The offset between the curves is for clarity. The FWHM increases by 3.6 meV upon a temperature change of 40 K. The inset shows a SEM image of some nanorods from the same batch. The scale bar is 50 nm.

5.2. EXPERIMENTAL METHOD

The experiments were performed in a home-built confocal microscope. The samples were mounted on a flow cell that allowed to raise the temperature of the medium up to 60 ^{o}C. A dry objective (Olympus 60× NA0.9) was employed to avoid the presence of a heat sink close to the observed area. To acquire white light scattering spectra the particles were immersed in index matching oil, therefore achieving a dark-field configuration without changes to the optics. Nanorods with average dimensions 20 nm × 50 nm, as shown in the inset of fig. 5.1 were spin coated on top of a clean coverslip. As a result, the number of dimers or clusters is below 1% of the observed diffraction-limited bright spots.

Spectra were recorded with an Acton 500-i spectrometer. Exposure times were on average of two seconds. This short time was possible because the collected scattered intensity is of the order of 10^5 counts per second with a laser-driven white light source (Energetiq).

Two different kinds of experiments were performed. Firstly spectra of a single nanorod were acquired continuously while varying the temperature in cycles, as shown in Figure 5.2. From 19 ^{o}C the temperature was increased to 60 ^{o}C and then freely cooled down. For the first analyzed particle the procedure was repeated three times in order to study fluctuations in the results given by the higher temperatures. Two more particles were studied in the same manner, but each was subject to one thermal cycle only. In every case, after each spectrum a background was recorded in the vicinity of the particle.

Secondly many particles were analyzed to improve the statistics of the results. In this set of experiments, each particle's spectrum was acquired consecutively. Also backgrounds in different regions of the sample were recorded. After the iteration on all particles was finished, the temperature was changed to a fixed value and the operation was repeated. In this way we have recorded the scattering spectrum of more than 200 particles at 9 different temperatures ranging from 19 ^{o}C to 58 ^{o}C. The first 5 measurements were done while increasing the temperature, while the last 4 were done when cooling down to

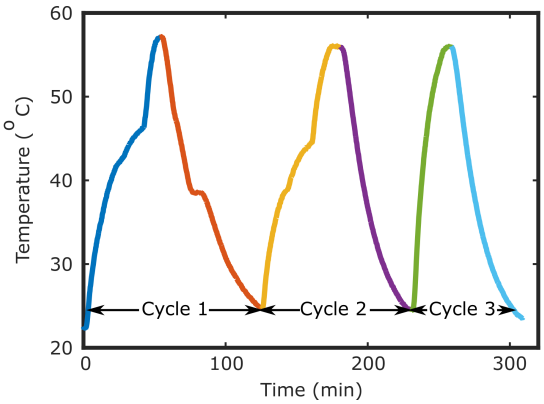

Figure 5.2: Example of the temperature cycle employed for studying a single gold nanorod. Spectra of the particle and of the background were acquired in intervals of approximately 10 s

room temperature.

In order to compensate for the drift of the setup while changing the temperature, a special computer program to control the setup was written. In the first set of experiments, it continuously refocused on the studied particle and triggered the spectrometer. The same program monitored and recorded the temperature of the flow-cell by measuring the resistance of a previously calibrated Pt100 thermometer, placed 1 mm away from the observed area. Only in the first cycle both the warming up and cooling down were done in steps, as can be seen in the Fig. 5.2, in order to slowly test the procedure.

In the second experiment, a reference particle was used for compensating the drift while changing temperature; the relative positions of the other particles were calculated accordingly. In every case an automatic refocusing procedure was applied before triggering the spectrometer, ensuring the correct positioning of the desired particle in the center of the beam. With this procedure, approximately 80 particles can be studied at 9 different temperatures in under 6 hours. Measuring the local temperature in the vicinity of the particles is important since the PID loop used to control the flow-cell temperature can have drifts of up to 4 ^{o}C.

5.3. RESULTS

The particle shown in Figure 5.1 was analyzed while continuously changing the temperature of the flow cell as described earlier. Figure 5.3 shows the FWHM (full width at half maximum) of the plasmon resonance as a function of temperature. Each row in the figure corresponds to every temperature cycle in Fig. 5.2, the first cycle on top and the last at the bottom. In every plot, the red dots show the part of the cycle with an increasing temperature. The blue crosses show the results when cooling down to room temperature.

In Fig. 5.3 it is possible to observe that during the first cycle there is a linear relationship between the plasmon resonance's width and temperature. In this cycle the plasmon broadens at a rate of 0.34 meV/ K. During the second cycle the broadening of the resonance is slightly less pronounced, at a rate of 0.23 meV/ K. During the third cycle the

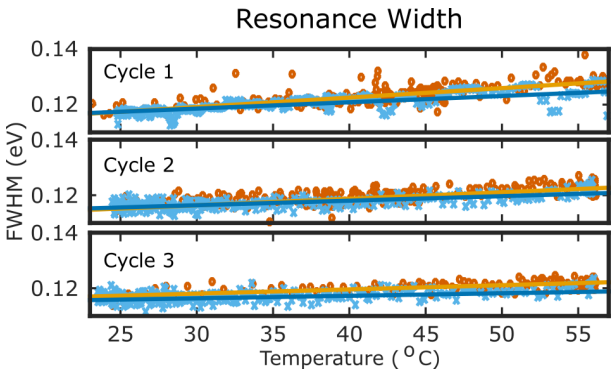

Figure 5.3: Plasmon width for one particle at varying temperatures. From top to bottom, each plot represents a thermal cycle, going from room temperature to 60 ^{o}C (red circles) and cooling down afterwards (blue crosses). It can be seen that after the second cycle the width increases reproducibly with temperature.

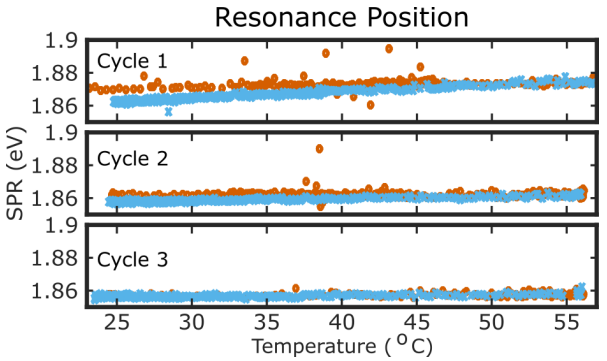

Figure 5.4: Resonance position for one particle at varying temperatures. From top to bottom, each plot represents a thermal cycle, going from room temperature to 60 ^{o}C (red circles) and cooling down afterwards (blue crosses). It can be seen that after the second cycle there is no variation of the plasmon resonance position, thus no reshaping of the particle.

broadening of the plasmon shows a rate of 0.15 meV/K. The results of the linear fittings of the FWHM of the plasmon while changing temperature are summarized in table 5.1. The values correspond to the slope of the line for the increasing and the decreasing part of the cycle separately. The cooling down part of the third cycle gives a measured rate of 0.09 meV/ K. This value is in good agreement with the expected broadening rate of 0.1 meV/ K reported earlier[28, 29] and expected from bulk gold measurements.

However the resonance damping rate is not the only parameter changing with temperature. Figure 5.4 shows that the resonance energy also shifts when changing the temperature of the immersion oil. The resonance goes from 1.869 eV at room temperature to 1.877 eV at 58 ^{o}C. More strikingly, when cooling down the resonance energy diminishes to 1.862 eV. The second cycle presents the same behavior but much less pronounced than during the first one. In the third cycle the resonance does not depend on temperature and is stable around 1.856 eV, indicating the the rods don't reshape significantly in our

Cycle	B_i(meV/K)	B_d(meV/K)	Particle	B_i(meV/K)	B_d(meV/K)
1	0.34	0.23	2	0.27	0.23
2	0.23	0.16	3	0.08	0.02
3	0.15	0.09			

Table 5.1: Summary of the results of the linear fittings for particles 1 (on the left). 2 and 3 (on the right). B_i and B_d are the results for the *i*ncreasing and *d*ecreasing part of the temperature cycles.

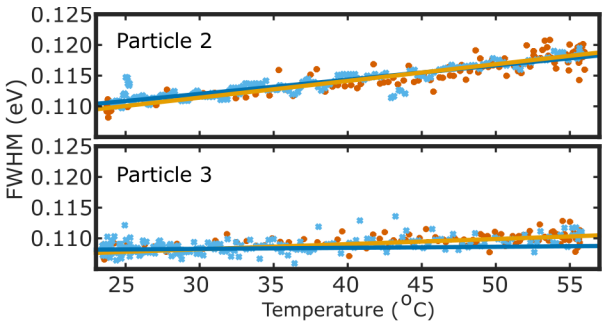

Figure 5.5: Plasmon width for two particles, going from room temperature to 60 ^{o}C (red circles) and cooling down afterwards (blue crosses). Both particles show a broadening of the plasmon proportional to temperature, but the rates are different.

conditions.

Normally plasmon shifts are related to changes in the refractive index of the medium surrounding the nanoparticles. This phenomenon is used, for instance, in photothermal imaging[39, 40] or in biosensors[14] as described in the introduction. The fact that in the first cycle there is a non-reversible plasmon shift suggests that either the medium or the surface of the particle (or both) changed in a permanent way after reaching higher temperatures. This can be due to a deterioration of the immersion oil, or to an adsorption/desorption of molecules from the particle's surface, effectively changing the refractive index in the surroundings of the nanorod. Discriminating these two mechanisms would require further studies that are out of the scope of this work.

Thermal reshaping of the nanoparticles can be ruled out since it would have induced a blue-shift of the resonance[41, 42], while we observe an overall red-shift. Moreover, the temperatures reached in this work are much lower than those needed for observing changes in shape of the nanorods. However, it is important to note that the plasmon broadening still occurs in the third temperature cycle when no resonance shift is observed. Therefore the broadening is not caused by changes in the medium but by intrinsic properties of the nanoparticles, as proposed in the introduction.

We performed the same experiment on two more particles. The measurements were carried on right after the third cycle of particle 1 in order to preserve the same experimental conditions and to avoid possible changes in the immersion oil as explained earlier. The surface plasmon resonance of both particles did not shift during their temperature cycles. This shows that the changes induced either on the surface of the particle or of the immersion oil at higher temperatures have a persistence of at least few hours.

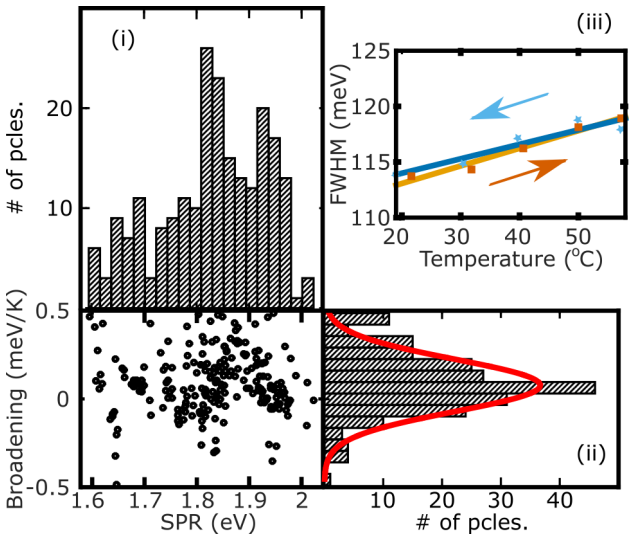

Figure 5.6: Plasmon broadening rate as a function of initial resonance position. Main panel shows the results for 220 different nanorods. Panel (i) is the histogram of the distribution of resonance energies found. Panel (ii) shows the distribution of broadening rates for all the particles and its fit by a gaussian as a solid red curve. Panel (iii) shows an example of the fitting for one particle; red squares correspond to increasing temperatures while blue crosses correspond to the decreasing.

The FWHM of the resonances of these two particles are shown in Figure 5.5. The slopes of every fit are summarized in table 5.1 on the right columns. Particle 2 shows a broadening rate higher than particle 1 while particle 3 shows a rate lower than expected. The heterogeneity in nanorod samples normally accounts for large variations in the observables. For instance quantum yield measurements[38] or the rate of chemical etching[43] of the surface of the particles show a broad distribution of values. To further investigate the differences between particles and to study if there is a relationship between the broadening rates and the plasmon resonance, we performed the same analysis on 220 different particles.

As described earlier, we acquired the scattering spectrum of several particles at different temperatures. The top right panel Figure 5.6 shows the result of the procedure for one of the particles as en example. The red squares show the FWHM of the plasmon resonance while increasing the temperature and the blue crosses correspond to the cooling down to room temperature. The linear fits have slopes of 0.14 meV/ K and 0.13 meV/ K respectively. Compared to the results shown in Figs. 5.3 and 5.5, spectra were not acquired continuously but after the temperature was stabilized at a certain value. At each temperature, spectra of several nanorods were acquired.

From the slopes of the linear fits of all the particles analyzed it is possible to construct the scatter plot of broadening rates and resonance energies for all the nanoparticles. This is shown in the bottom left panel of Figure 5.6. The particles analyzed had resonances varying from 1.6 eV to 2 eV, and the distribution of energies is shown in the top left histogram of Fig.5.6. The most frequent resonance is around 1.81 eV. The distribution of

resonance energies is also an indication of the dispersion of shapes of the samples and is inherent to wet chemical synthesis methods.

The broadening rates of the 220 studied particles are summarized in the histogram at the bottom right in fig. 5.6. The gaussian fit of the distribution has the center at 0.08 meV/ K with a standard deviation of 0.3 meV/ K. This is in good agreement with the expected broadening rate of 0.1 meV/ K. The measurements were performed after some thermal cycles and no change in the plasmon resonance energy was observed while increasing or decreasing the temperature. This implies that the broadening rates differ from particle to particle because of inherent properties and not because of differences generated by the immersion oil used.

From Figure 5.6 it is possible to discard any significant dependence of the plasmon broadening rate on the plasmon's resonance position if this is kept below the interband transition energy. The model proposed in the introduction accounts for the broadening of the plasmon in terms of the electron-phonon coupling in gold and can account for the average behavior observed. It is important to note, however, that particles with resonances to the red normally have narrower plasmons[30]. Therefore the sensitivity of the broadening will be higher for particles with lower resonance energies.

The distribution of rates shown in Fig. 5.6 also includes particles that show a narrowing of the plasmon resonance while the temperature increases. Approximately 27% of the studied nanorods present a negative broadening rate. The model of electron-phonon coupling proposed in this work does not account for this phenomenon, nor for the different broadening rates for different particles. It is possible that the uncertainty in the determination of the plasmon width is responsible in part for this. The expected plasmon width change with a temperature increase of 40 K is of about 4 meV, or 4% of the FWHM of the resonance of the particles.

5.4. CONCLUSIONS

Measuring temperature at the nanoscale is challenging. Available techniques rely on spectral changes of fluorophores[44] or quantum dots[1, 9]. Here we show that scattering properties of gold nanoparticles can also be used as temperature sensors. One of the main advantages is that the scattering cross section of gold nanoparticles is on the order of 10^3 nm^2, and therefore the powers needed for measuring the spectrum as well as the integration times can be low.

Electron-phonon coupling in gold is one of the parameters responsible for the broad plasmonic resonance of nanoparticles. This is also the only parameter that depends strongly on temperature and can be modeled with a simple linear relation for temperatures in the range that we studied, between 293 K and 350 K. It is therefore expected that the plasmon width depends linearly on temperature as was shown in this work.

Particles were studied in detail, acquiring continuously spectra while increasing and decreasing the immersion medium's temperature and showed a broadening of their resonances with various rates. The electron-phonon coupling model does not allow us to explain this behavior; however we have also observed that the resonance energy changes with temperature and a persistent red-shift is observed. This is attributed to changes in the refractive index of the medium surrounding the particles, either due to the immersion oil changing in a non reversible way or to some modification of the surface chemistry

of the particles (for instance because of adsorption of molecules present in the oil). The plasmon shift however disappears after some thermal cycles, but the plasmon broadening remains.

In the situation when no resonance shift with increasing or decreasing temperature is observed, we have investigated the differences in the broadening rates from particle to particle. Spectra of more than 200 nanorods were studied, allowing us to discard a possible relationship of the rates with the resonance position. It was found that the broadening rates have a distribution centered around 0.08 meV/ K, while the value expected from bulk measurements is 0.1 meV/ K[33]. The standard deviation of the distribution of rates is 0.3 meV/ K.

The model proposed in this work cannot account for the distribution of rates observed. However it has to be noted that when working with gold nanoparticles, the distribution of values of selected quantities can be of up to one order of magnitude. For example, quantum yield measurements[38], surface chemistry[43], plasmon induced reactions[45] are some of the examples of the high variability observed from particle to particle. This variability also makes single-particle studies important since many of the phenomena can be hidden in bulk measurements[34].

With the measured average broadening rate, reaching sensitivities of 1 K imply detecting changes in the plasmon width of 0.08 meV, less than 0.1% of the total width. The error in the fitting of the scattering spectrum is mainly given by the amount of light collected. Longer exposure times can lead to lower errors and therefore higher sensitivities. On the other hand, detecting several particles at the same time can lead to increasing the temperature sensitivity. Without any previous calibration, the broadening of the plasmon can be used at best to detect temperature changes, but not the absolute temperature of the sample.

REFERENCES

[1] J.-M. Yang, H. Yang, and L. Lin, *Quantum Dot Nano Thermometers Reveal Heterogeneous Local Thermogenesis in Living Cells,* ACS Nano **5**, 5067 (2011).

[2] X. Huang, P. K. Jain, I. H. El-Sayed, and M. A. El-Sayed, *Determination of the Minimum Temperature Required for Selective Photothermal Destruction of Cancer Cells with the Use of Immunotargeted Gold Nanoparticles,* Photochem. Photobiol. **82**, 412 (2006).

[3] L. R. Hirsch, R. J. Stafford, J. A. Bankson, S. R. Sershen, B. Rivera, R. E. Price, J. D. Hazle, N. J. Halas, and J. L. West, *Nanoshell-mediated near-infrared thermal therapy of tumors under magnetic resonance guidance.* Proc. Natl. Acad. Sci. U. S. A. **100**, 13549 (2003), arXiv:0008204 [cond-mat] .

[4] J. L. West and N. J. Halas, *Engineered nanomaterials for biophotonics applications: improving sensing, imaging, and therapeutics.* Annu. Rev. Biomed. Eng. **5**, 285 (2003).

[5] H. Ma, P. Tian, J. Pello, P. M. Bendix, and L. B. Oddershede, *Heat Generation by Irradiated Complex Composite Nanostructures.* Nano Lett. **14**, 612 (2014).

[6] X. Huang, P. K. Jain, I. H. El-Sayed, and M. A. El-Sayed, *Plasmonic photothermal therapy (PPTT) using gold nanoparticles,* Lasers Med. Sci. **23**, 217 (2008).

[7] D. Hone, P. Walker, and R. Evans-Gowing, *Generation of cytotoxic singlet oxygen via phthalocyanine-stabilized gold nanoparticles: A potential delivery vehicle for photodynamic therapy,* Langmuir , 2985 (2002).

[8] Y. Cheng, A. C. Samia, J. D. Meyers, I. Panagopoulos, B. Fei, and C. Burda, *Highly efficient drug delivery with gold nanoparticle vectors for in vivo photodynamic therapy of cancer,* J. Am. Chem. Soc. **130**, 10643 (2008).

[9] R. Tanimoto, T. Hiraiwa, Y. Nakai, Y. Shindo, K. Oka, N. Hiroi, and A. Funahashi, *Detection of Temperature Difference in Neuronal Cells.* Sci. Rep. **6**, 22071 (2016).

[10] J. S. Donner, S. a. Thompson, C. Alonso-Ortega, J. Morales, L. G. Rico, S. I. C. O. Santos, and R. Quidant, *Imaging of Plasmonic Heating in a Living Organism,* ACS Nano **7**, 8666 (2013).

[11] P. Ruijgrok, N. Verhart, P. Zijlstra, a. Tchebotareva, and M. Orrit, *Brownian Fluctuations and Heating of an Optically Aligned Gold Nanorod,* Phys. Rev. Lett. **107**, 1 (2011).

[12] J. Trojek, L. Chvátal, and P. Zemánek, *Optical alignment and confinement of an ellipsoidal nanorod in optical tweezers: a theoretical study.* J. Opt. Soc. Am. A. Opt. Image Sci. Vis. **29**, 1224 (2012).

[13] a. S. Urban, M. Fedoruk, M. R. Horton, J. O. Rädler, F. D. Stefani, and J. Feldmann, *Controlled nanometric phase transitions of phospholipid membranes by plasmonic heating of single gold nanoparticles.* Nano Lett. **9**, 2903 (2009).

[14] P. Zijlstra, P. M. R. Paulo, and M. Orrit, *Optical detection of single non-absorbing molecules using the surface plasmon resonance of a gold nanorod.* Nat. Nanotechnol. **7**, 379 (2012).

[15] M. A. Beuwer, M. W. J. Prins, and P. Zijlstra, *Stochastic protein interactions monitored by hundreds of single-molecule plasmonic biosensors,* Nano Lett. **15**, 3507 (2015).

[16] K. M. Spillane, J. Ortega-Arroyo, G. de Wit, C. Eggeling, H. Ewers, M. I. Wallace, and P. Kukura, *High-speed single-particle tracking of GM1 in model membranes reveals anomalous diffusion due to interleaflet coupling and molecular pinning.* Nano Lett. **14**, 5390 (2014).

[17] J. Conde, J. Rosa, J. M. de la Fuente, and P. V. Baptista, *Gold-nanobeacons for simultaneous gene specific silencing and intracellular tracking of the silencing events.* Biomaterials **34**, 2516 (2013).

[18] J. a. Schuller, E. S. Barnard, W. Cai, Y. C. Jun, J. S. White, and M. L. Brongersma, *Plasmonics for extreme light concentration and manipulation.* Nat. Mater. **9**, 193 (2010).

[19] C. Leduc, S. Si, J. Gautier, M. Soto-Ribeiro, B. Wehrle-Haller, A. Gautreau, G. Giannone, L. Cognet, and B. Lounis, *A highly specific gold nanoprobe for live-cell single-molecule imaging.* Nano Lett. **13**, 1489 (2013).

[20] K. R. Catchpole and A. Polman, *Plasmonic solar cells.* Opt. Express **16**, 21793 (2008).

[21] P. Zijlstra and M. Orrit, *Single metal nanoparticles: optical detection, spectroscopy and applications,* Reports Prog. Phys. **74**, 106401 (2011).

[22] M. Beversluis, A. Bouhelier, and L. Novotny, *Continuum generation from single gold nanostructures through near-field mediated intraband transitions,* Phys. Rev. B **68**, 1 (2003).

[23] M. B. Mohamed, V. Volkov, S. Link, and M. A. El-Sayed, *The 'lightning' gold nanorods: fluorescence enhancement of over a million compared to the gold metal,* Chem. Phys. Lett. **317**, 517 (2000).

[24] S. T. Sivapalan, B. M. Devetter, T. K. Yang, T. van Dijk, M. V. Schulmerich, P. S. Carney, R. Bhargava, and C. J. Murphy, *Off-resonance surface-enhanced Raman spectroscopy from gold nanorod suspensions as a function of aspect ratio: not what we thought.* ACS Nano **7**, 2099 (2013).

[25] H. Yuan, S. Khatua, P. Zijlstra, M. Yorulmaz, and M. Orrit, *Thousand-fold enhancement of single-molecule fluorescence near a single gold nanorod.* Angew. Chem. Int. Ed. Engl. **52**, 1217 (2013).

[26] S. Khatua, P. M. R. Paulo, H. Yuan, A. Gupta, P. Zijlstra, and M. Orrit, *Resonant plasmonic enhancement of single-molecule fluorescence by individual gold nanorods.* ACS Nano **8**, 4440 (2014).

[27] J. Prasad, I. Zins, R. Branscheid, J. Becker, A. H. R. Koch, G. Fytas, U. Kolb, and C. Sönnichsen, *Plasmonic Core-Satellite Assemblies as Highly Sensitive Refractive Index Sensors,* J. Phys. Chem. C **119**, 5577 (2015).

[28] M. Liu, M. Pelton, and P. Guyot-Sionnest, *Reduced damping of surface plasmons at low temperatures,* Phys. Rev. B **79**, 035418 (2009).

[29] A. Konrad, F. Wackenhut, M. Hussels, A. J. Meixner, and M. Brecht, *Temperature Dependent Luminescence and Dephasing of Gold Nanorods,* J. Phys. Chem. C **117**, 21476 (2013).

[30] C. Sönnichsen, T. Franzl, T. Wilk, G. von Plessen, J. Feldmann, O. Wilson, and P. Mulvaney, *Drastic Reduction of Plasmon Damping in Gold Nanorods,* Phys. Rev. Lett. **88**, 077402 (2002).

[31] C. Novo, D. Gomez, J. Perez-Juste, Z. Zhang, H. Petrova, M. Reismann, P. Mulvaney, and G. V. Hartland, *Contributions from radiation damping and surface scattering to the linewidth of the longitudinal plasmon band of gold nanorods: a single particle study,* Phys. Chem. Chem. Phys. **8**, 3540 (2006).

[32] M. Hu, C. Novo, A. Funston, H. Wang, H. Staleva, S. Zou, P. Mulvaney, Y. Xia, and G. V. Hartland, *Dark-field microscopy studies of single metal nanoparticles: understanding the factors that influence the linewidth of the localized surface plasmon resonance,* J. Mater. Chem. **18**, 1949 (2008).

[33] J. A. McKay and J. A. Rayne, *Temperature dependence of the infrared absorptivity of the noble metals,* Phys. Rev. B **13**, 673 (1976).

[34] S. Link and M. a. El-Sayed, *Size and Temperature Dependence of the Plasmon Absorption of Colloidal Gold Nanoparticles,* J. Phys. Chem. B **103**, 4212 (1999).

[35] C. Kittel, *Introduction to solid state physics* (Wiley, 1995).

[36] R. Sundararaman, P. Narang, A. S. Jermyn, W. a. Goddard III, and H. a. Atwater, *Theoretical predictions for hot-carrier generation from surface plasmon decay,* Nat. Commun. **5**, 5788 (2014).

[37] A. Manjavacas, J. G. Liu, V. Kulkarni, and P. Nordlander, *Plasmon-Induced Hot Carriers in Metallic Nanoparticles,* ACS Nano **8**, 7630 (2014).

[38] M. Yorulmaz, S. Khatua, P. Zijlstra, A. Gaiduk, and M. Orrit, *Luminescence quantum yield of single gold nanorods.* Nano Lett. **12**, 4385 (2012).

[39] S. Berciaud, D. Lasne, G. Blab, L. Cognet, and B. Lounis, *Photothermal heterodyne imaging of individual metallic nanoparticles: Theory versus experiment,* Phys. Rev. B **73**, 045424 (2006).

[40] A. Gaiduk, M. Yorulmaz, P. V. Ruijgrok, and M. Orrit, *Room-Temperature Detection of a Single Molecule's Absorption by Photothermal Contrast,* Science (80-.). **330**, 353 (2010).

[41] Y. Liu, E. N. Mills, and R. J. Composto, *Tuning optical properties of gold nanorods in polymer films through thermal reshaping,* J. Mater. Chem. **19**, 2704 (2009).

[42] Y. Horiguchi, K. Honda, Y. Kato, N. Nakashima, and Y. Niidome, *Photothermal reshaping of gold nanorods depends on the passivating layers of the nanorod surfaces,* Langmuir **24**, 12026 (2008).

[43] A. Carattino, S. Khatua, and M. Orrit, *In situ tuning of gold nanorod plasmon through oxidative cyanide etching,* Phys. Chem. Chem. Phys. **18**, 15619 (2016).

[44] C. F. Chapman, Y. Liu, G. J. Sonek, and B. J. Tromberg, *THE USE OF EXOGENOUS FLUORESCENT PROBES FOR TEMPERATURE MEASUREMENTS IN SINGLE LIVING CELLS,* Photochem. Photobiol. **62**, 416 (1995).

[45] L. Osinkina, S. Carretero-Palacios, J. Stehr, A. a. Lutich, F. Jäckel, and J. Feldmann, *Tuning DNA Binding Kinetics in an Optical Trap by Plasmonic Nanoparticle Heating.* Nano Lett. , 1 (2013).